Pharmaceutical Sciences Asia

Pharm Sci Asia 2026; 53(2), 112-121

DOI:10.29090/psa.2026.02.25.8814

Research Article

Ivermectin ameliorates cyst progression in polycystic kidney disease rats and renal cell-derived cysts via suppression of chloride secretion

Kanlayanee Tonum[1], Nipitpon Srimai[2], Sunhapas Soodvilai[2]*

[1]Department of Physiology, Faculty of Pharmacy, Mahidol University, Bangkok, 10400, Thailand
[2]Research Center of Transporter Protein for Medical Innovation, Department of Physiology, Faculty of Science, Mahidol University, Bangkok, 10400, Thailand

ABSTRACT

Polycystic kidney disease (PKD) is a genetic disorder characterized by the growth of numerous fluid-filled cysts in the kidneys. Ivermectin is an antiparasitic drug that has been reported to function as an agonist of the farnesoid X receptor (FXR). Activation of FXR has previously been shown to attenuate cyst progression. In the present study, we evaluated the pharmacological effects of ivermectin on renal cyst progression *in vivo* in a rat model of PKD and *in vitro* in renal cell-derived cysts. Daily subcutaneous administration of ivermectin (0.5 mg/kg body weight) for 12 weeks significantly reduced the kidney weight–to–body weight ratio and improved renal function in PKD rats compared with vehicle-treated controls. In addition, treatment with 2 µM ivermectin significantly inhibited Madin–Darby canine kidney (MDCK) cell-derived cyst formation by 31±5.3% compared to vehicle-treatment. These effects were associated with suppressed cell proliferation and reduced phosphorylation of extracellular signal-regulated kinases (ERK)1/2. In addition, ivermectin significantly attenuated *in vitro* cyst growth by 13±3.0% compared with control. This inhibitory effect on cyst growth was associated with reduced cystic fibrosis transmembrane conductance regulator (CFTR)– and TMEM16A-mediated chloride secretion by 36±3.1% and 12±2.8%, respectively, compared with control. Collectively, these findings demonstrate that ivermectin inhibits renal cyst progression both *in vivo* and *in vitro*, supporting its potential as a pharmacological modulator of cyst growth in PKD.

Keywords:
Ivermectin; Repurposing drug; Chloride secretion; Kidney; Farnesoid X receptor

1. INTRODUCTION

Polycystic kidney disease (PKD) is a genetic disorder characterized by the development of numerous fluid-filled cysts that progressively impair kidney function [1]. Autosomal dominant polycystic kidney disease (ADPKD), the most common form of PKD, is caused by mutations in the genes encoding polycystin-1 (PC-1) and polycystin-2 (PC-2) [2]. Dysfunction of the PC1/PC2 complex in renal epithelial cells leads to increased intracellular cAMP levels, which stimulates cell proliferation and cyst expansion[3]. cAMP-driven signaling activates sequential components of the Ras-Raf-MEK-ERK pathway, thereby enhancing proliferation[4, 5]. In addition, cAMP promotes cyst progression by cAMP-stimulated transepithelial Cl^- transport [4, 5]. In PKD cyst epithelia, Cl^- enters cells via Na^+-K^+-$2Cl^-$ cotransporter coupled with Na^+/K^+-ATPase at the basolateral side [6]. Cl^- transports into the luminal side via the cystic fibrosis transmembrane conductance regulator (CFTR) Cl^- channel [7, 8] and calcium-activated chloride channels (CaCCs) [7]. Among the CaCCs, TMEM16A plays a role in the accumulation of fluid in the renal cysts [9-11]. Ivermectin is an FDA-approved drug for treatment of parasitic conditions [12, 13].

***Corresponding author:**
* Sunhapas Soodvilai Email: Sunhapas.soo@mahidol.ac.th

Besides its established anti-helminthic properties, ivermectin has gained renewed scientific interest due to emerging evidence of its broader pharmacological activities. Recent studies have reported that ivermectin inhibits the proliferation of several tumor cell types by modulating multiple signaling pathways implicated in cancer progression [14]. Moreover, antiviral activities of ivermectin have been demonstrated against multiple viruses, including HIV-1, dengue virus [15] and SARS-CoV-2 [16, 17]. In addition to its pharmacological activities, ivermectin has been identified as a novel and selective agonist of the farnesoid X receptor (FXR). Treatment of wild-type mice fed a high-fat diet with ivermectin reduced serum glucose and cholesterol levels; these effects were abolished in FXR knockout mice [18]. These data support that ivermectin regulates metabolic homeostasis in an FXR-dependent manner. We previously demonstrated that FXR activation attenuates Cl^- secretion and suppresses cyst growth in renal collecting duct cells by inhibiting CFTR-dependent Cl^- transport [19]. Based on these observations, the present study investigated the therapeutic effects of ivermectin on cyst progression in PKD rats. In addition, the underlying mechanisms of ivermectin action were elucidated, with a particular focus on CFTR- and TMEM16A-mediated Cl^- secretion.

2. MATERIALS AND METHODS

2.1. Chemicals

Ivermectin (for *in vitro* experiments), forskolin (FSK), MTT reagent, adenosine triphosphate (ATP), amiloride, human insulin, sodium selenite, and apo-transferrin, hyaluronidase were purchased from Sigma-Aldrich (MO, USA). Type I collagenase was purchased from Worthington Biochemical (New Jersey, USA). [Arg8]-vasopressin (AVP) was purchased from the Ferring International Center (Prex, Switzerland). PureCol (purified bovine collagen) was purchased from Advanced BioMatrix (CA, USA). Fetal bovine serum (FBS), DMEM/F12 media, trypsin-EDTA, penicillin, and streptomycin were purchased from Gibco (NY, USA). The iScript cDNA synthesis kit was obtained from Bio-Rad Laboratories (Bangkok, Thailand). The LUNA® SYBR Green universal master mix was obtained from New England BioLabs (Frankfurt, Germany). Antibodies against extracellular signal regulated kinases (ERK)1/2, p-ERK1/2, and Actin were obtained from Cell Signaling (Massachusetts, USA). All the other chemicals used in this study were of analytical grade and obtained from commercial sources.

2.2. Animals and experimental protocol

The animal protocol no. MUSC65-022-615 has been approved by the Institutional Animal Care and Use Committee (MUSC–IACUC). Male PCK rats were obtained from Charles River Japan (Tokyo, Japan). The PCK rat is an inherited model of polycystic kidney disease (PKD) that arose spontaneously in the Crj:CD/SD strain and exhibits progressive renal cyst formation with histopathological features closely resembling those of human PKD [20]. Heterozygous PCK:SD male rats, which carry one mutant allele but do not develop renal cysts, were used as non-cystic controls. Animals were housed under standard laboratory conditions with free access to water and a standard diet.

Rats were randomly divided into three groups: (1) heterozygous PCK:SD rats receiving vehicle (control group); (2) PCK rats receiving vehicle; and (3) PCK rats receiving ivermectin (0.5 mg/kg BW). The ivermectin dose was selected based on established safety profiles and repeated-dose toxicology data in rodents, ensuring a significant safety margin for the 12-week study duration [21]. The subcutaneous route was chosen to ensure stable drug bioavailability and minimize animal handling stress during the 12-week treatment period.

Starting at 8 weeks of age, ivermectin (Baymec™, 1% w/v; oil-based formulation; Elanco Animal Health, Korea) or vehicle was administered once daily via subcutaneous injection. The formulation was diluted to 0.5 mg/mL using a solvent mixture of propylene glycol, PEG 400, and sterile water. The detailed treatment timeline is illustrated in Figure 1A. At the end of the treatment period (20 weeks of age), rats were anesthetized with an intraperitoneal injection of xylazine (15 mg/kg) and zolazepam–tiletamine (Zoletil®, 40 mg/kg). Blood was collected via intracardiac puncture for biochemical analysis, and kidneys were excised and weighed to determine the kidney-to-body weight (2KW/BW) ratio. Kidney tissues were then either fixed in 10% buffered formaldehyde for histological evaluation or snap-frozen in liquid nitrogen for molecular analyses. Renal cystic area, kidney function parameters, and inflammatory cytokine levels were then assessed.

2.3. Cell culture

MDCK cells were cultured in DMEM/F12 medium supplemented with 10% FBS, penicillin/streptomycin, and insulin-transferrin-selenium at 37ºC in a humidified incubator with 95% O_2 and 5% CO_2.

2.4. Primary renal collecting duct cell culture

The primary renal collecting duct cells were isolated from rat IMCD as previously described [22]. The renal medulla was minced and incubated with digestion medium containing serum-free DMEM, 0.2% of type I collagenase and hyaluronidase, and 0.125% trypsin-EDTA at 37 °C for 60 minutes with shaking. After

incubation, the cells suspension was centrifuged at 1,500 rpm for 10 minutes. To eliminate non-collecting duct cells, the supernatant was replaced by serum-free DMEM (100 mOsm/kgH_2O) for 20 minutes. Cells were then centrifuged at 1,500 rpm for 10 minutes, the cells were collected and resuspended in the complete medium (DMEM; 10% FBS, 20 ng/ml epidermal growth factor, insulin-transferin-selenium, and 100 U/ml penicillin G-streptomycin sulfate). Cell suspensions were seeded onto Snapwell inserts for 10-14 days. The inserts with a high transepithelial resistance (resistance > 1,000 $\Omega \cdot cm^2$) were selected for electrophysiological study.

2.5. Cell viability assay

MDCK cells were treated with vehicle (0.1% DMSO) or ivermectin at several concentrations for 24, 48, or 72 h. Following treatment, cell viability was assessed using the MTT assay. Briefly, 0.5% MTT reagent was added to each well and incubated for 4 h at 37 °C. The medium was then removed, and the formazan crystals were dissolved in 100% DMSO. Absorbance was measured at 570 nm using a microplate reader. Cell viability was expressed as a percentage of the vehicle-treated control.

2.6. Electrophysiological analysis

High-resistance cell monolayers cultured on Snapwell inserts were mounted into the Ussing chamber filled with physiological buffer (in mM; 117 NaCl, 4.7 KCl, 25 $NaHCO_3$, 1.2 $MgSO_4$, 2.5 $CaCl_2$, 1.2 KH_2PO_4, and 11 D-glucose) at 37°C and pH of 7.4. To measure Cl^- secretion, short-circuit current (I_{SC}) under inhibition of ENaC-mediated Na^+ current was measured by a VC600 voltage clamp (Physiologic Instruments). Measurement of CFTR- and TMEM16A-mediated Cl^- secretion were determined by adding vasopressin (AVP; 20 nM) to the basolateral side and adenosine triphosphate (ATP; 100 µM) to the apical side, respectively.

2.7. Cell proliferation assay

MDCK cells cultured on a 24-well plate were incubated with vehicle or ivermectin for 72 hours under a humidified atmosphere at 37 ºC. The cells were removed by trypsinization with 0.25% trypsin-EDTA for 15 minutes. Complete media containing trypan blue was added to inhibit trypsin activity. The live cells were counted on a hematocytometer under a light microscope for comparison between the vehicle and treatment groups.

2.8. Cyst formation and growth

To perform MDCK cell-derived cyst formation, MDCK cells (400–600 cells/well) were grown in collagen gel as previously described [23]. Briefly, MDCK cell suspension containing 10 µM forskolin with or without ivermectin was added to a 24-well plate containing collagen gel that composed of 10% 10x minimum essential medium (MEM), 27 mM $NaHCO_3$, 10 mM HEPES, and penicillin/streptomycin (adjusted pH 7.4 with NaOH). The cells were then cultured in a humidified incubator under 95% O_2 and 5% CO_2. The medium was changed every two days. To quantify cyst formation, on day 6 after seeding, the number of cysts (with diameters > 50 µm) and non-cyst cell colonies were counted by a phase-contrast light inverted microscope (10× magnification). For the assessment of cyst growth, individual cysts with an initial diameter ≥ 50 µm (at least 20 cysts) were identified on day 6 and monitored throughout the treatment period. These selected cysts were treated with either vehicle or ivermectin for an additional 6 days. Increases in cyst diameter were documented using a phase-contrast microscope at 10× magnification. Images were acquired at 2-day intervals and subsequently analyzed. Cyst diameters were measured using ImageJ software, and the growth rate was calculated as the change in diameter relative to the baseline measurement on day 6.

2.9. Histological processing and cystic quantification

Harvested kidney tissues were fixed in 10% neutral buffered formalin, and processed for paraffin embedding. Paraffin-embedded kidneys were sectioned at 5 µm thickness and stained with hematoxylin and eosin (H&E) according to standard protocols. Total kidney sections were captured using an Olympus Cx33 inverted microscope (Olympus, Tokyo, Japan) at 4× magnifications. Cystic burden was quantified by measuring the cystic area relative to the total kidney area using ImageJ software, and the results were normalized to the control group and expressed as cyst area (% of control).

2.10. Measurement of inflammatory cytokines in the kidney

The kidney tissue was ground and then lysed with ice-cold tissue lysis buffer. The inflammation-mediating cytokines, including MCP-1 and TNF-α, were determined using the MILLIPLEX® MAP Rat Cytokine/Chemokine Magnetic Bead Panel-Immunology Multiplex Assays (#RECYTMAG-65K) (Millipore®, Massachusetts, USA).

2.11. qPCR analysis

Total RNA was extracted from kidney tissues of PCK rats using TRIzol reagent according to the manufacturer's instructions. The purity and concentration

of RNA were determined by using a Nanodrop spectrophotometer. Next, RNA was converted into cDNA by an iScript cDNA synthesis kit (Bio-Rad), and the mRNA expression level was quantified using a LUNA® SYBR Green universal master mix (BioLabs®) in the qTOWER^{3}G Real-Time qPCR Thermal Cycler (Analytik Jena). Relative quantification was determined using the $2^{-\Delta\Delta CT}$ method. All primers were designed based on sequences in the National Center for Biotechnology Information (NCBI) database. The following primers were used: rat OST-α (forward, 5'-TAGCATCTGCCCTCCAATTCA-3' and reverse, 5'-GTGCCAGCATCCTTACCGTG-3'); rat OST-β (forward, 5'-GGTGGGGCTTTGTCTAACCT-3' and reverse, 5'-GCCTGGGCATCCTAAGAGAG-3'); and rat GAPDH (forward, 5'-AGAGTTAATGCCGCCCCTTAC-3' and reverse, 5'-GCCATCAACGACCCCTTCA-3').

2.12. Western blotting

Total protein lysates of MDCK cells were separated by 10% SDS-polyacrylamide gel electrophoresis and transferred onto nitrocellulose membranes. The membranes were blocked with 10% non-fat milk for 2 hours, followed by incubation with primary antibodies against ERK1/2, p-ERK1/2, and actin (1:1,000 dilution) overnight at 4 °C. The membranes were washed and incubated with a horseradish peroxidase-conjugated secondary antibody for 1 hour. Expression intensities were detected by the Azure 600 Gel Imaging System (Azure Biosystem, Inc., California, USA) using Electro-Chemi-Luminescence (ECL) system.

2.13. Statistical analysis

Data are shown as mean ± SD Statistical differences were determined using student t-test or a one-way ANOVA followed by Tukey's test. A *P*-value less than 0.05 was considered statistically significant.

3. RESULTS

3.1. Effect of ivermectin on renal cyst progression in PKD rats

We previously reported that activation of FXR suppressed CFTR-mediated Cl^- secretion in renal collecting ducts and attenuates renal cyst progression [19]. We investigated whether ivermectin, an antiparasitic drug known to act as an FXR agonist, exerts inhibitory effects on renal cyst development in PCK rats (cystic rats). The experimental protocol is schematically represented in Figure 1A. PCK rats were administered daily subcutaneous injections of either vehicle or 0.5 mg/kg BW ivermectin from 8 to 20 weeks of age. To confirm FXR activation, we assessed the expression of its target genes. Ivermectin treatment led to significant upregulation of OST-β mRNA expression, a known FXR target [24], whereas OST-α levels remained unchanged (Fig. 1B). Ivermectin treatment was well tolerated throughout the 12-week period, as indicated by stable body weight (Fig. 1C) and the absence of gross abnormalities in major organs (data not shown). Furthermore, ivermectin treatment significantly reduced the 2KW/BW ratio and the relative cystic area compared with the vehicle-treated group (Fig. 1D). Regarding renal function, cystic PCK rats exhibited impairment as indicated by elevated blood urea nitrogen (BUN) levels compared to non-cystic (heterozygous) rats, although plasma creatinine levels did not show a significant rise at this stage. Notably, ivermectin treatment improved renal function in cystic rats, evidenced by a significant reduction in BUN levels (Fig. 2A). Additionally, ivermectin administration significantly reduced the level of the renal inflammatory cytokine MCP-1 compared with the vehicle-treated group, and led to a decreasing trend for TNF-α (Fig. 2B).

3.2. Effect of ivermectin on MDCK-derived cyst growth

The effect of ivermectin on viability of MDCK cells was determined. As illustrated in Fig. 3A, treatment with ivermectin at concentrations ≤2.5 μM for 72 h did not significantly affect cell viability, whereas 5 μM ivermectin markedly reduced cell viability. Therefore, 2 μM ivermectin was chosen for subsequent experiments to avoid cytotoxic effects. We next examined whether ivermectin inhibits cyst formation. MDCK cells embedded in collagen gel were treated with vehicle or 2 μM ivermectin for six days, followed by quantification of cyst colonies. Treatment with ivermectin significantly reduced the number of cysts compared with vehicle-treated controls (Fig. 3B). To determine whether the inhibitory effect of ivermectin on cyst formation was associated with altered cell proliferation, MDCK cells were treated with vehicle or 2 μM ivermectin for 72 h. Ivermectin treatment resulted in a significant reduction in cell number compared with vehicle-treated cells (Fig. 3B), indicating suppressed cell proliferation. Given the central role of MAPK signaling in regulating cell proliferation, we next evaluated the effect of ivermectin on ERK activation. As shown in Fig. 3C, treatment with ivermectin for 48 h significantly reduced ERK1/2 phosphorylation, while total ERK levels remained unchanged, compared with vehicle-treated cells. Finally, we investigated whether ivermectin affects renal cyst growth. MDCK-derived cysts were treated with vehicle or 2 μM ivermectin,

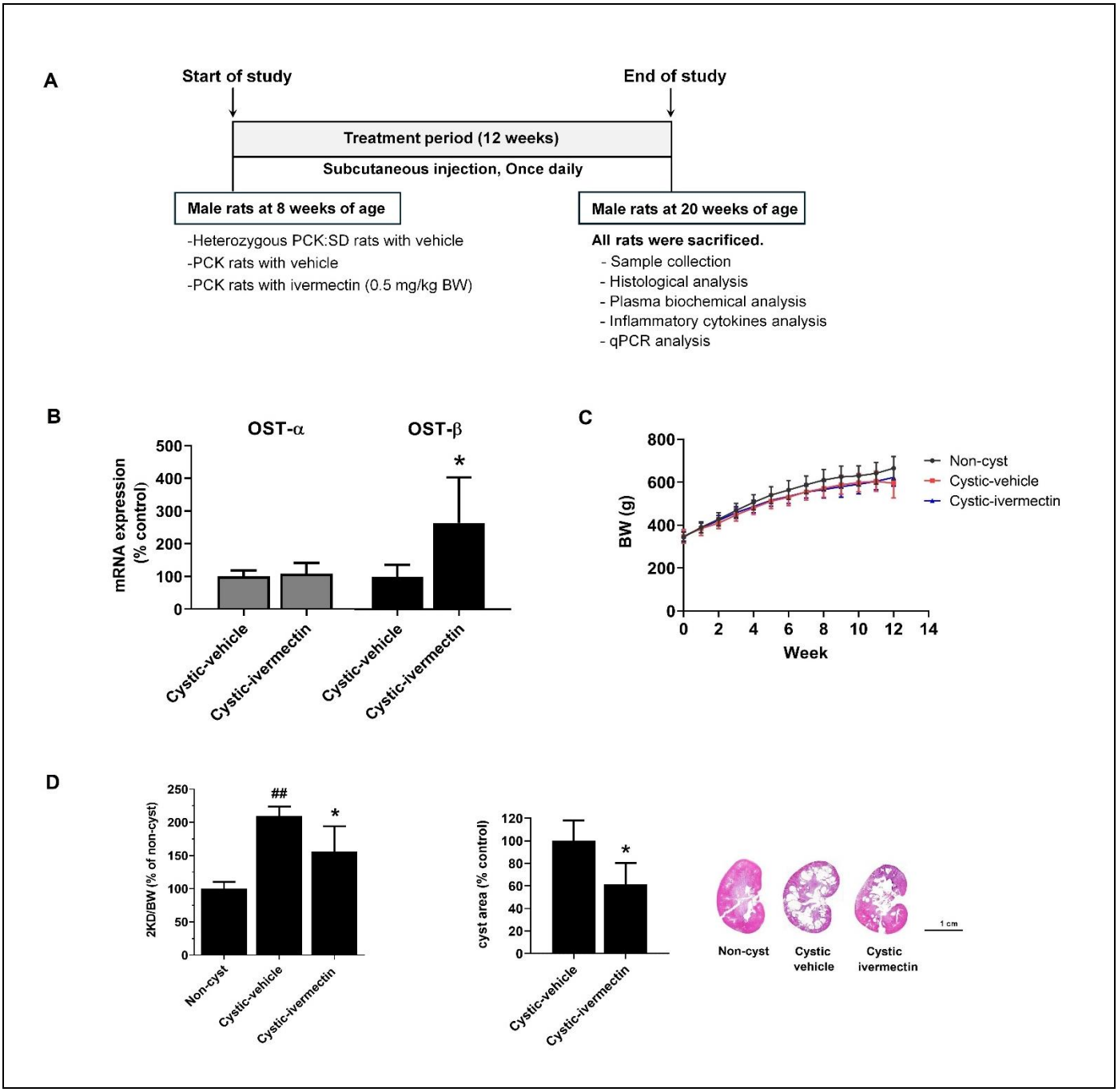

Figure 1. Experimental design and the effect of ivermectin on renal cyst progression in PCK rats. (A) Schematic diagram illustrating the experimental design and treatment timeline. PCK rats were administered vehicle or ivermectin 0.5 mg/kg BW starting at 8 weeks of age and continued for 12 weeks until 20 weeks of age. Ivermectin or vehicle was administered once daily via subcutaneous injection. (B) mRNA expression of OST-α and, OST-β (C) Body weight (BW) measured over the 12-week period, (D) Kidney weight to body weight ratio (2KW/BW) and relative cystic area (expressed as % of vehicle control). Data are presented as mean ± SD (n = 7 for vehicle group; n = 6 for ivermectin group). Scale bar = 1 cm. $^{*}P < 0.05$ vs. vehicle-treated rats; $^{\#\#}P < 0.001$ vs. non-cyst rats.

and cyst diameters were monitored over a six-day period. As shown in Fig. 3D, ivermectin treatment significantly attenuated cyst growth compared with vehicle treatment.

3.3. Effect of ivermectin on chloride secretion in renal collecting duct cells

Cl^- secretion plays a crucial role in renal cyst progression in PKD [8, 25, 26]. We next assessed the effects of ivermectin on CFTR- and TMEM16A-mediated Cl^- secretion in renal collecting duct cells. MDCK cell monolayers grown on Snapwell inserts were incubated with vehicle or 2 µM ivermectin for 48 hours. As shown in Fig. 4A, incubation with 2 µM ivermectin significantly decreased AVP- and ATP-stimulated Cl^- secretion, indicating inhibition of CFTR and TMEM16A activity, respectively. In addition, we examined the pharmacological effect of ivermectin on Cl^- secretion in

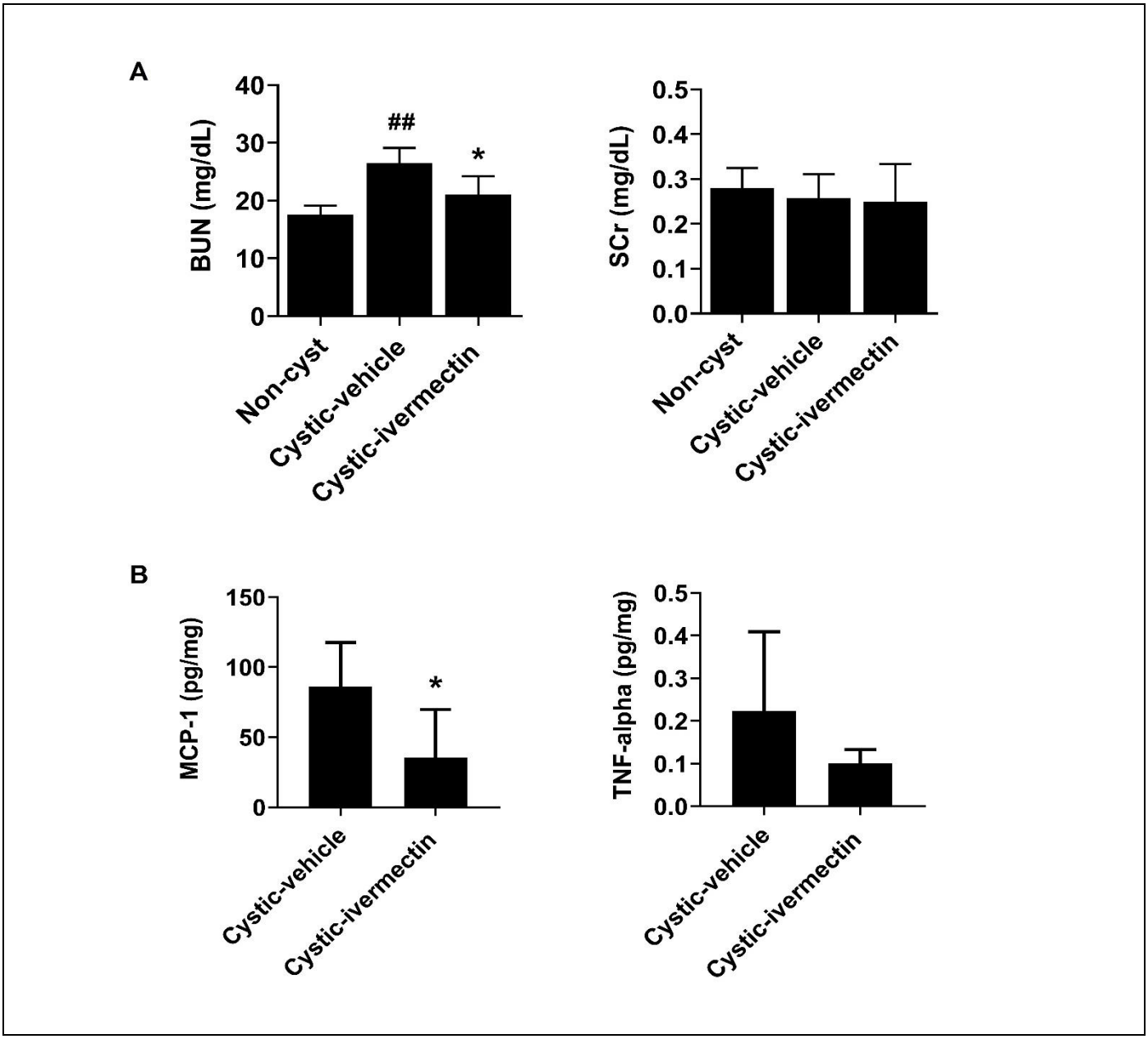

Figure 2. Effect of ivermectin on renal function and inflammatory cytokines in PCK rats. (A) BUN and serum creatinine levels, and (B) renal inflammatory cytokines (MCP-1 and TNF-α) in non-cystic rats (n=5), PCK rats treated with vehicle (n=7) or ivermectin 0.5 mg/kg BW (n=6) for 12 weeks. Data are presented as mean ± SD. $^{*}P < 0.05$ vs. vehicle-treated cystic rats; $^{\#\#}P < 0.001$ vs. non-cyst rats.

primary culture of rat renal collecting duct cells. Treatment with 2 μM ivermectin significantly decreased AVP-induced Cl^- secretion compared with vehicle-treated cells (Fig. 4B).

4. DISCUSSION

Although the pathophysiology of PKD progression is well characterized at the cellular level, ongoing research continues to elucidate additional signaling pathways and to develop targeted therapeutic strategies. Our previous study revealed that activation of FXR inhibits Cl^- secretion and subsequently suppresses cyst growth in MDCK cell-derived cysts [19]. In the present study, we investigated the therapeutic potential of ivermectin, an antiparasitic drug [14, 18, 27] that has been reported to exhibit FXR agonistic activity [18, 28-30], as a repurposing candidate for the treatment of PKD.

This study demonstrates the inhibitory effects of ivermectin on renal cyst progression. Histopathological examination of PCK rat kidneys showed numerous fluid-filled cysts predominantly located in the renal medulla. Kidney function declined, as indicated by increased BUN levels, while serum creatinine remained unchanged [31-33]. Our findings show that ivermectin significantly reduced kidney weight and renal cyst burden compared with vehicle-treated PCK rats. Treatment of PCK rats with ivermectin also

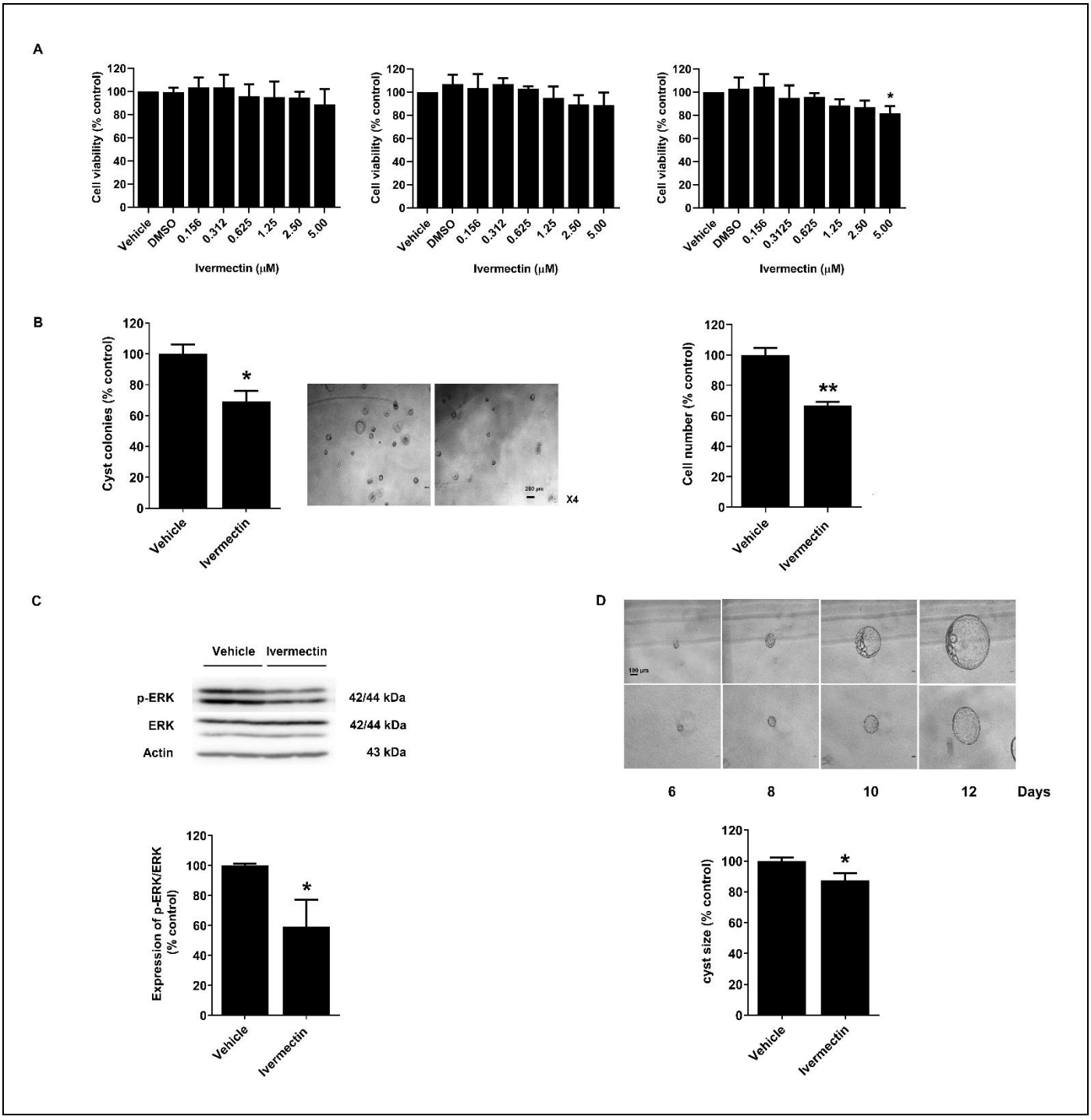

Figure 3. Effect of ivermectin on MDCK-derived cyst formation. (A) Cell viability of MDCK cells treated with vehicle or ivermectin at final concentrations ranging from 0.156 to 5 μM for 24, 48, and 72 h. Ivermectin was dissolved in DMSO and applied to cells at the indicated concentrations. (B) Cyst colony formation expressed as percentage of vehicle-treated control during 6 days of culture in collagen gel, together with MDCK cell number (% control) after 72 h of treatment with 2 μM ivermectin. (C) Representative immunoblots and quantitative analysis of p-ERK normalized to total ERK, expressed as percentage of vehicle-treated control after 48 h of treatment. (D) Cyst growth observed by phase-contrast microscope and photographed for 6 days (on Day 12) at 10x magnification. Data are presented as means ± SD from three to six independent experiments. $^{*}P < 0.05$ and $^{**}P < 0.001$ compared with vehicle-treated control.

improved renal function, as evidenced by a reduction in BUN levels. Inflammation has increasingly been recognized as an early and active contributor to PKD pathogenesis [34]. Notably, experimental evidence indicates that the expression of pro-inflammatory cytokines, including monocyte chemoattractant protein-1 (MCP-1), are elevated in PKD. Elevated urinary and renal tissue levels of MCP-1 have been shown to correlate with disease progression in patients with PKD [34-37]. Accordingly, we investigated whether the beneficial effects of ivermectin on renal function were associated with modulation of inflammatory signaling. Interestingly,

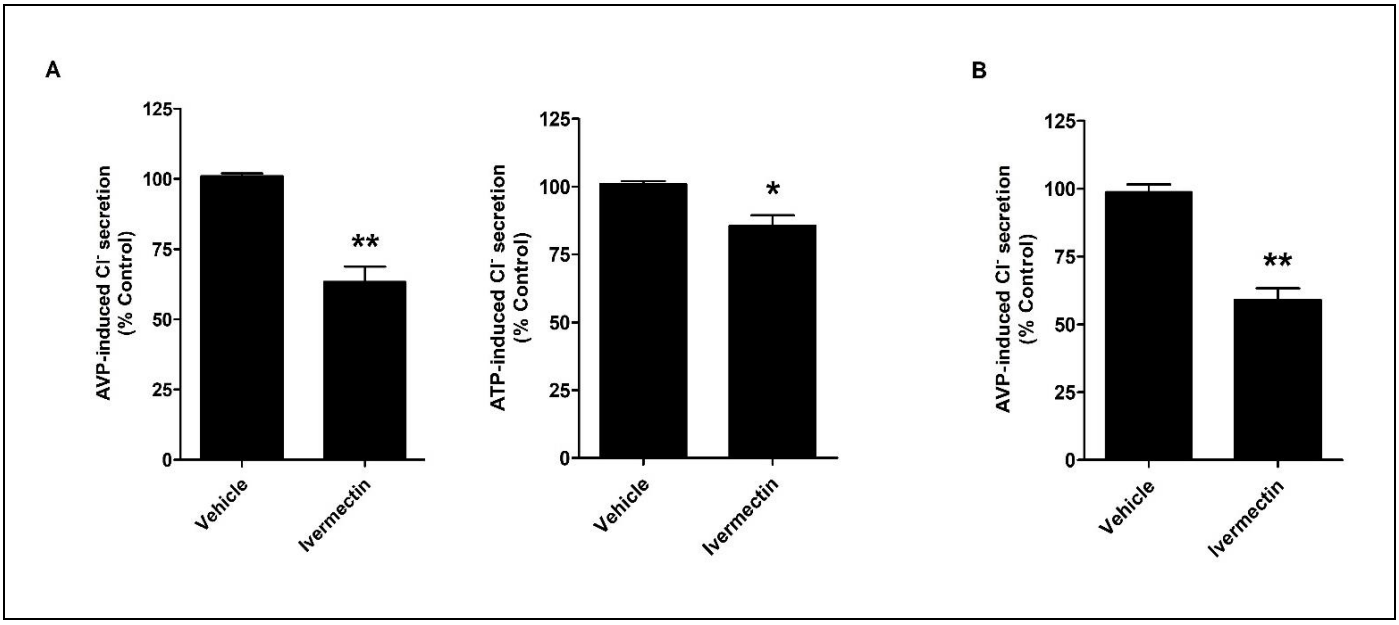

Figure 4. Effect of ivermectin on Cl^- secretion. (A) AVP-induced and ATP-induced Cl^- secretion in MDCK cell monolayers following treatment with vehicle or 2 µM ivermectin for 48 h. (B) AVP-induced Cl^- secretion in primary rat IMCD cells following treatment with vehicle or 2 µM ivermectin for 24 h. Data are expressed as mean ± SD as percentages of control from three independent experiments in MDCK cell and seven independent experiments in primary rat IMCD cells. $^*P < 0.05$ and $^{**}P < 0.001$ compared with vehicle-treated cells.

ivermectin markedly reduced MCP-1 levels in the renal tissue of PCK rats, and TNF-α levels exhibited a downward trend following treatment. Given the established role of MCP-1–mediated inflammatory cell recruitment in promoting cyst growth, these findings suggest that the anti-inflammatory effects of ivermectin may be biologically relevant to cyst suppression. However, because inflammation and cyst burden are tightly interrelated with PKD, the present study does not establish a direct causal relationship. It therefore remains possible that the observed anti-inflammatory changes are secondary to reduced cyst burden and overall disease severity. Consistent with this interpretation, the improvement in renal function observed in PCK rats is likely mediated by multiple mechanisms beyond inflammation alone.

Next the mechanism by which ivermectin decreased renal cyst area and kidney weight was investigated *in vitro* using the MDCK cell-derived cyst model. Treatment with ivermectin decreased MDCK cell-derived cyst formation without affecting cell viability, suggesting that its inhibitory effect was not attributable to cytotoxicity. Given the evidence that renal cyst development is driven in part by increased epithelial cell proliferation [3, 4], we evaluated whether ivermectin influences this process. Indeed, ivermectin markedly suppressed cell proliferation in MDCK cells, and this reduction was accompanied by decreased phosphorylation of ERK1/2, an essential regulator of proliferative signaling [4, 5]. The ERK1/2 signaling pathway has been extensively implicated in cyst expansion in PKD. Hyperactivation of the Ras–Raf–MEK–ERK cascade contributes to abnormal epithelial proliferation and progressive cyst growth [38, 39]. In this study, the suppression of ERK1/2 phosphorylation by ivermectin treatment was closely associated with reduced MDCK cell proliferation and diminished cyst formation, suggesting that direct or indirect inhibition of ERK-dependent proliferative signaling is one of its underlying mechanisms.

In addition to inhibiting cyst formation, ivermectin also attenuated forskolin-induced cyst enlargement, indicating a direct effect on cyst growth. Since transepithelial Cl^- secretion is essential for fluid accumulation and cyst expansion,[7-11] we hypothesized that the inhibitory effect of ivermectin may be mediated, at least in part, by suppression of Cl^- secretion. Electrophysiological analyses demonstrated that ivermectin inhibited both, AVP- and ATP-stimulated Cl^- secretion mediated by CFTR and TMEM16A, respectively. Accordingly, the suppression of cyst growth by ivermectin can be partially explained by reduced Cl^- transport and the consequent limitation of fluid influx into the cyst lumen. Chloride secretion represents the primary driving force for cyst fluid accumulation [40], the dual inhibition of CFTR- and TMEM16A-mediated chloride transport by ivermectin is likely to exert a substantial functional impact on cyst expansion. Simultaneous modulation of both channels may therefore provide an advantage over strategies targeting a single chloride transport pathway, thereby contributing to the robust suppression of cyst growth observed in this study.

Consistent with this notion, our previous work demonstrated that FXR activation reduces CFTR function through transcriptional regulation of the

channel [19]. Although ivermectin has been reported to function as an FXR agonist, a limitation of the present study is that FXR involvement was not directly examined using pharmacological inhibition or genetic approaches. Therefore, the contribution of FXR signaling to the observed effects of ivermectin remains speculative. Additional studies are also warranted to determine whether the regulation of CFTR and TMEM16A by ivermectin occurs directly or indirectly through FXR-dependent signaling pathways.

5. CONCLUSIONS

Ivermectin suppresses renal cyst progression in renal cell–derived cysts and an animal model of PKD. The inhibitory effect of ivermectin is associated with reduced chloride secretion–mediated fluid accumulation through inhibition of CFTR and TMEM16A. These findings support the therapeutic potential of ivermectin for the treatment of PKD.

6. ACKNOWLEDGEMENTS

This research project was supported by the National Research Council of Thailand and Mahidol University (Grant N42A660361 to S.S.). We would like to thank Dr. David N. Sheppard for providing the MDCK cells.

Author contribution

K.T. and S.S. conceived and designed the study and wrote the manuscript. K.T. and N.S., performed the experiments and collected and analyzed the data. K.T., N.S., and S.S. interpreted the data. All the authors approved the manuscript for publication.

Funding

This work was funded by the National Research Council of Thailand and Mahidol University (Grant N42A660361 to Sunhapas Soodvilai).

Conflict of interest

None to declare.

Ethics approval

None to declare.

Article info:
Received December 7, 2025
Received in revised form February 18, 2026
Accepted February 28, 2026

REFERENCES

1. Hou X, Mrug M, Yoder BK, Lefkowitz EJ, Kremmidiotis G, D'Eustachio P, et al. Cystin, a novel cilia-associated protein, is disrupted in the cpk mouse model of polycystic kidney disease. J Clin Invest. 2002;109(4):533-40.
2. Chebib FT, Torres VE. Autosomal dominant polycystic kidney disease: core curriculum 2016. Am J Kidney Dis. 2016;67(5):792-810.
3. Zhou J. Polycystins and primary cilia: primers for cell cycle progression. Annu Rev Physiol. 2009;71(1):83-113.
4. Hanaoka K, Guggino WB. cAMP regulates cell proliferation and cyst formation in autosomal polycystic kidney disease cells. J Am Soc Nephrol. 2000;11(7):1179-87.
5. Yamaguchi T, Pelling JC, Ramaswamy NT, Eppler JW, Wallace DP, Nagao S, et al. cAMP stimulates the *in vitro* proliferation of renal cyst epithelial cells by activating the extracellular signal-regulated kinase pathway. Kidney Int. 2000;57(4):1460-71.
6. Magenheimer BS, John PLS, Isom KS, Abrahamson DR, De Lisle RC, Wallace DP, et al. Early embryonic renal tubules of wild-type and polycystic kidney disease kidneys respond to camp stimulation with cystic fibrosis transmembrane conductance regulator/Na^{+}· K^{+}, 2Cl− co-transporter–dependent cystic dilation J Am Soc Nephrol. 2006;17(12):3424-37.
7. Nilius B, Droogmans G. Amazing chloride channels: an overview. Acta Physiol Scand. 2003;177(2):119-47.
8. Li H, Findlay IA, Sheppard DN. The relationship between cell proliferation, Cl− secretion, and renal cyst growth: a study using CFTR inhibitors. Kidney Int. 2004;66(5):1926-38.
9. Cabrita I, Buchholz B, Schreiber R, Kunzelmann K. TMEM16A drives renal cyst growth by augmenting Ca^{2+} signaling in M1 cells. J Mol Med (Berl). 2020;98(5):659-71.
10. Cabrita I, Kraus A, Scholz JK, Skoczynski K, Schreiber R, Kunzelmann K, et al. Cyst growth in ADPKD is prevented by pharmacological and genetic inhibition of TMEM16A *in vivo*. Nat Commun. 2020;11(1):4320.
11. Buchholz B, Faria D, Schley G, Schreiber R, Eckardt K-U, Kunzelmann K. Anoctamin 1 induces calcium-activated chloride secretion and proliferation of renal cyst–forming epithelial cells. Kidney Int. 2014;85(5):1058-67.
12. Kaur B, Blavo C, Parmar MS. Ivermectin: A multifaceted drug with a potential beyond anti-parasitic therapy. Cureus. 2024;16(3).
13. Elgart GW, Meinking TL. Ivermectin. Dermatol Clin. 2003;21(2):277-82.
14. Juarez M, Schcolnik-Cabrera A, Dueñas-Gonzalez A. The multitargeted drug ivermectin: from an antiparasitic agent to a repositioned cancer drug. Am J Cancer Res. 2018;8(2):317.
15. Wagstaff KM, Sivakumaran H, Heaton SM, Harrich D, Jans DA. Ivermectin is a specific inhibitor of importin α/β-mediated nuclear import able to inhibit replication of HIV-1 and dengue virus. Biochem J. 2012;443(3):851-6.
16. Caly L, Druce JD, Catton MG, Jans DA, Wagstaff KM. The FDA-approved drug ivermectin inhibits the replication of SARS-CoV-2 *in vitro*. Antiviral Res. 2020;178:104787.
17. Rajter JC, Sherman MS, Fatteh N, Vogel F, Sacks J, Rajter J-J. Use of ivermectin is associated with lower mortality in hospitalized patients with coronavirus disease 2019: the ivermectin in COVID nineteen study. Chest. 2021;159(1):85-92.
18. Jin L, Feng X, Rong H, Pan Z, Inaba Y, Qiu L, et al. The antiparasitic drug ivermectin is a novel FXR ligand that regulates metabolism. Nat Commun. 2013;4(1):1937.
19. Srimai N, Tonum K, Soodvilai S. Activation of farnesoid X receptor retards expansion of renal collecting duct cell-derived cysts via inhibition of CFTR-mediated Cl–secretion. Am J Physiol Renal Physiol. 2024;326(4):F600-F10.
20. Lager DJ, Qian Q, Bengal RJ, Ishibashi M, Torres VE. The pck rat: a new model that resembles human autosomal dominant polycystic kidney and liver disease. Kidney Int. 2001;59(1):126-36.
21. Descotes J. Medical Safety of Ivermectin. Expert Review report IMMUNOSAFE CONSULTANCE. 2021;120.
22. Soodvilai S, Jia Z, Yang T. Hydrogen peroxide stimulates chloride secretion in primary inner medullary collecting duct

cells via mPGES-1-derived PGE2. Am J Physiol Renal Physiol. 2007;293(5):F1571-F6.
23. Tonum K, Jintanapanya P, Srimai N, Chabang N, Soodvilai S. Metabolites of lansoprazole inhibit CFTR-mediated Cl– transport and retard cyst progression. J Pharmacol Sci. 2025;51(3):2025044.
24. Boyer JL, Trauner M, Mennone A, Soroka CJ, Cai S-Y, Moustafa T, et al. Upregulation of a basolateral FXR-dependent bile acid efflux transporter OSTα-OSTβ in cholestasis in humans and rodents. Am J Physiol Gastrointest Liver Physiol. 2006;290(6):G1124-G30.
25. Sullivan LP, Wallace DP, Grantham JJ. Chloride and fluid secretion in polycystic kidney disease. J Am Soc Nephrol. 1998;9(5):903-16.
26. Buchholz B, Schley G, Faria D, Kroening S, Willam C, Schreiber R, et al. Hypoxia-inducible factor-1α causes renal cyst expansion through calcium-activated chloride secretion. J Am Soc Nephrol. 2014;25(3):465-74.
27. Campbell WC. Lessons from the history of ivermectin and other antiparasitic agents. Annu Rev Anim Biosci. 2016;4(1):1-14.
28. Jin L, Wang R, Zhu Y, Zheng W, Han Y, Guo F, et al. Selective targeting of nuclear receptor FXR by avermectin analogues with therapeutic effects on nonalcoholic fatty liver disease. Sci. Rep. 2015;5(1):17288.
29. Chen IS, Kubo Y. Ivermectin and its target molecules: shared and unique modulation mechanisms of ion channels and receptors by ivermectin. J Physiol. 2018;596(10):1833-45.
30. Tian S-y, Chen S-m, Pan C-x, Li Y. FXR: structures, biology, and drug development for NASH and fibrosis diseases. Acta Pharmacol Sin. 2022;43(5):1120-32.
31. Lyman JL. Blood urea nitrogen and creatinine. Emerg Med Clin North Am. 1986;4(2):223-33.
32. Hosten AO. BUN and creatinine. Clinical methods: The history, physical, and laboratory examinations 3rd edition. 1990.
33. Salazar JH. Overview of urea and creatinine. Lab. Med 2014;45(1):e19-e20.
34. Karihaloo A. Role of inflammation in polycystic kidney disease. Exon Publications. 2015:335-73.
35. Derouiche S, Chetehouna S, Boulaares I, Frahtia A, Ahmed OZ, Rouag O, et al. A review of the pathophysiology of cysts diseases and their therapeutic strategies. WSEAS Trans. Biol. Biomed. 2025;22(1):1-13.
36. Song CJ, Zimmerman KA, Henke SJ, Yoder BK. Inflammation and fibrosis in polycystic kidney disease. Results Probl Cell Differ. 2017:323-44.
37. Ta MH, Harris DC, Rangan GK. Role of interstitial inflammation in the pathogenesis of polycystic kidney disease. Nephrology. 2013;18(5):317-30.
38. Parker E, Newby L, Sharpe C, Rossetti S, Streets A, Harris P, et al. Hyperproliferation of PKD1 cystic cells is induced by insulin-like growth factor-1 activation of the Ras/Raf signalling system. Kidney Int. 2007;72(2):157-65.
39. Parker MI, Nikonova AS, Sun D, Golemis EA. Proliferative signaling by ERBB proteins and RAF/MEK/ERK effectors in polycystic kidney disease. Cell Signal. 2020;67:109497.
40. Zhou X, Torres VE. Emerging therapies for autosomal dominant polycystic kidney disease with a focus on cAMP signaling. Front Mol Biosci. 2022;9:981963.